All responses will be presented in Times New Roman font. The responses will appear in black, while revisions made to the manuscript will be highlighted in blue.

Shunyu Yao

Major Comment:

Scientific Significance

I want to raise some concerns regarding the key finding presented in this manuscript, as one major part of the result overlaps significantly with a 2022 Science paper. (Shen et al., 2022) In the previous publication, the effect of NO has already been discussed, and mechanisms have been thoroughly evaluated. This manuscript does show innovation through the no NO condition, which was not present in previous research, and the addition of pinonaldehyde control, which offered a concrete conclusion to the formation pathway. However, the overlap in key conclusions with prior work is substantial. I will list some overlapping parts in conclusion from both the manuscript and publication.

2022 Paper: "the formation rate of C10H15OX•-related HOM is mainly affected by the NO concentration." "In this study, RO• are mainly formed by the alkoxy step (RO2• + NO ➔ RO• + NO2), whose reaction rate depends on the current NO concentration, while the ring opening is especially fast with a typical rate >106 s−1. As a consequence, the formation rate of C10H15OX-related HOM is mainly affected by the NO concentration."

Manuscript conclusion: "C10H15Ox··-related HOM exhibits a strong dependence on NO levels and can only be formed in significant amounts in the presence of NO."

2022 Paper: "time series of C10H17OX•-related HOM are similar at low and high NO."

Manuscript result: "The C10H17O7· peroxy radicals exhibit a rapid formation rate and a high molar yield in α-pinene photooxidation, and the formation is not strongly dependent on NO concentration."

2022 Paper also made a time-based analysis to assess whether pinonaldehyde oxidation will result in C10H15OX formation and ruled out such possibility as pinonaldehyde takes longer to form than H-abstraction product. The manuscript used a similar approach by cluster definition and had the same conclusion.

Pinonaldehyde oxidation control was a novel approach which was not present in the 2022 paper. This control allows readers to directly compare yield of HOM produced from pinonaldehyde oxidation and H-abstraction, in which case H-abstraction had much better yield. This combined with cluster time difference

provides stronger evidence of why C10H15Ox does not originate from pinonaldehyde oxidation. There are other novel approaches in this manuscript, such as using both amine-CIMS and nitrate-CIMS to capture a broader range of products, including less-oxygenated species.

The conclusion also addresses one important finding, stating that the contribution of the H-abstraction related products observed in this study is 70 % lower than that reported in the 2022 paper. Authors contributed this difference to inlet, stating that multi-scheme ionization inlet was used for this study, while the 2022 paper used Eisele type inlet. The lower value reported in this manuscript could be an interesting path to pursue, but no direct explanation was given.

The scientific significance would benefit from clearer positioning relative to prior work, particularly the 2022 study. The study applies largely novel experimental approaches to a system whose core conclusions are broadly consistent with prior literature. The scope of detection was widened, and additional control experiments have been done to enhance conclusions. I believe it's an excellent addition to this field of study, but the conclusion does seem to repeat the older paper.

Responses:

We thank Shunyu Yao for his extensive community comment in general and for this thoughtful comment in particular. We agree that the current abstract and conclusion are focusing on the confirmation of the findings reported by Shen et al. (2022), rather than emphasizing the novelty of the present work. The motivation of this work arises from discrepancies between Shen et al. (2022) and other studies (Berndt et al., 2016; Berndt, 2021; Xu et al., 2019), in which the role of the H-abstraction pathway was considered negligible. The objective of this work is not to reproduce the previous results, but to validate and constrain the findings presented in Shen et al. (2022), and to extend the mechanistic understanding of H-abstraction by systematically exploring related experimental conditions in a well-controlled steady-state chamber (Baker et al., 2024).

In this context, the main novelties of the present study are as follows:

1. A fully NO-free condition has been included, allowing a direct comparison between regimes without and with NO presented, which provides stronger constraints on the role of NO for the H-abstraction pathway in HOM formation. NO-free in this study refers to conditions where the measured NO concentration was below the detection limit, in our case below 50 ppt.
2. The combined use of CIMS with nitrate and amine ionization modes enables a broader coverage of the product distributions, particularly of less oxygenated intermediates (e.g., C10H15NO4). In the

case α-pinene photooxidation, the H-abstraction channel can result in an opening of the six-membered ring and subsequently to the formation of peroxy radicals, which are potentially linked to the above-mentioned intermediates like C10H15NO4.

3. To constrain the importance of the H-abstraction channel and to deepen the mechanistic understanding, we also conducted pinonaldehyde photooxidation experiments under comparable conditions as in the α-pinene experiments, which helps to further evaluate the current understanding and to assess the contribution of pinonaldehyde oxidation, a concurrent pathway, to the observed C10H15Ox-related HOM formation in the α-pinene system.

We have therefore revised and extended the manuscript to clarify these points and to better emphasize the new aspects and the constraints provided by the present study, which distinguish it from previous works.

Revised Abstract:

Highly oxygenated organic molecules (HOM) are efficiently formed via autooxidation during ·OH-initiated oxidation of α-pinene. We investigated the relative contributions of ·OH-addition and hydrogen (H)-abstraction to HOM formation from α-pinene photooxidation under varying NO conditions. HOM molecules were detected by a nitrate chemical ionization mass spectrometer (CIMS). In the absence of NO, $C_{10}H_{17}O_x$· peroxy radicals and related termination products (e.g. $C_{10}H_{18}O_x$) dominated the HOM spectrum, accounting for more than 70% of total HOM. The presence of NO substantially altered HOM products, particularly by the rapid formation of $C_{10}H_{15}O_x$·-related HOM like $C_{10}H_{15}NO_8$. The ratio of $C_{10}H_{15}NO_x$ to $C_{10}H_{17}NO_x$ increased significantly from 0.34 to 0.84 as the RO_2· loss rate via reaction with NO increased from 0.18 s^{-1} to 1.06 s^{-1}. Under high-NO conditions, $C_{10}H_{15}O_x$·-related HOM contributed up to 34% to total HOM from α-pinene oxidation systems. H-abstraction channel was proven to be the source of $C_{10}H_{15}O_x$·-related HOM. Fuzzy c-means clustering indicated that $C_{10}H_{15}O_x$·-related HOM exhibited the fastest formation rate among the identified HOM groups, consistent with first-generation products. Comparison with pinonaldehyde oxidation, obtained by normalizing HOM yields to pinonaldehyde turnover, suggests that pinonaldehyde contributed ~5% of HOM in α-pinene systems, excluding secondary oxidation as the dominant source. Detection of $C_{10}H_{15}NO_4$ under high-NO conditions by propylamine-CIMS is indicator for formation of $C_{10}H_{15}O_3$· peroxy radicals, formed by alkoxy radical decomposition and six-membered ring opening in H-abstraction channel. This study highlights the role of the H-abstraction pathway in OH-initiated α-pinene oxidation under NO-influenced conditions and provides new constraints on detailed HOM formation mechanisms.

Revised Conclusions:

In this study a series of photooxidation experiments was conducted under varying NO levels to investigate the effect of NO on the $C_{10}H_{15}O_x$·-related HOM formation in the α-pinene photooxidation system, and to unravel potential formation pathways of these products. The chemical system was brought to a steady state in the dark. Afterwards, reactions were initiated by photolyzing H_2O_2. We focused on early reaction stages (the first hundreds of seconds), during which RO_2· + NO reactions and RO_2· autoxidation reactions dominate the fate of the RO_2·. $C_{10}H_{17}O_x$·-related HOM are dominantly formed via the ·OH·-addition pathway. Product distributions, potential formation pathways, and rates of $C_{10}H_{17}O_x$·-related HOM have been widely and extensively studied (Berndt, 2021; Xu et al., 2019), and our findings on $C_{10}H_{17}O_x$·-related HOM formation are consistent with previous studies. However, potential formation pathways, distributions, and NO dependence of $C_{10}H_{15}O_x$·-related compounds derived from H-abstraction channel were missing systematic exploration so far.

To constrain the potential contribution of H-abstraction to HOM formation, regimes with and without NO were directly compared, and a separate experiment of pinonaldehyde oxidation under similar conditions was performed. Additionally, measurements by Amine-CIMS were used to detect less oxygenated products. Since the photolysis of H_2O_2 was utilized to produce ·OH radicals O_3 did not accumulate during the early reaction stages; therefore, ozonolysis did not interfere with the ·OH pathways. FCM analysis proves that the dominant species in the $C_{10}H_{15}NO_x$ family, $C_{10}H_{15}NO_8$ and $C_7H_9NO_8$, can be distinguished from other species by their fast formation rates in the presence of NO. Pinonaldehyde oxidation can only contribute ~ 5% to HOM formation in α-pinene oxidation systems. Therefore, neither ozonolysis nor secondary oxidation can explain the significant formation of $C_{10}H_{15}O_x$·-related HOM, which points to H-abstraction from α-pinene by ·OH being the most likely formation pathway.

As illustrated in ***Figure S12*** and ***Figure S16,*** the contribution of the H-abstraction pathway to HOM formation increases with elevated NO levels compared to the OH-addition pathway. The ratios between major $C_{10}H_{15}O_x$·-related HOM and $C_{10}H_{17}$Ox·-related HOM rise with increasing NO concentrations. The ratios of $C_{10}H_{15}O_x$· peroxy radicals to $C_{10}H_{17}O_x$· peroxy radicals are 0.06, 0.83, and 1.42 under NO-free, low-NO, and high-NO conditions, respectively. Similarly, the ratio of $C_{10}H_{15}NO_x$ to $C_{10}H_{17}NO_x$ increases from 0.34 to 0.84 when NO levels increase from low to high. The sum of major $C_{10}H_{15}O_x$·-related closed-shell HOM products ($C_{10}H_{14}O_x$, $C_{10}H_{15}NO_x$ and $C_{10}H_{16}O_x$) contributes 24% and 34% under low-NO and high-NO conditions, while being negligible under NO-free conditions.

The comparison between α-pinene and pinonaldehyde was highlighted:

HOM formation in each system was normalized by the pinonaldehyde turnover and discussion was extended. To calculate the turnover, ·OH radicals were estimated by box model simulations. The revised manuscript was attached as follows:

To assess the potential contribution of pinonaldehyde oxidation to the formation of $C_{10}H_{15}O_x$·-related HOM, pinonaldehyde photooxidation experiments were conducted under NO-free and high-NO conditions, analogous to conditions applied in the α-pinene systems (***Table 1***). Time series of α-pinene and its oxidation product pinonaldehyde during the first 30 min of the α-pinene (high-NO) experiment are shown in Figure ***5(a-1).*** The corresponding turnovers of α-pinene and pinonaldehyde are presented in Figure ***5(a-1).*** Similarly, the concentration of pinonaldehyde and its turnover during the pinonaldehyde (high-NO) experiment are shown in Figure ***5(a-2).*** ·OH concentrations were estimated using model simulations.

During early stage, the average pinonaldehyde turnover was 8.9×10^6 molecules cm^{-3} s^{-1} under pinonaldehyde (high-NO) condition, approximately 6 times higher than the turnover (1.5×10^6 molecules cm^{-3} s^{-1}) under α-pinene (high-NO) condition. To facilitate comparison between the two experiments, we calculated the pinonaldehyde turnover for both experiments and compared it to obtain the ratio between the high-NO α-pinene and pinonaldehyde experiment (hereafter referred to as the pinonaldehyde turnover ratio). Signals measured in the pinonaldehyde experiment were subsequently normalized by this ratio to account for differences in the pinonaldehyde turnover between the two experimental systems. The distributions of major $C_{10}H_{15}O_x$·-related products observed during the high-NO α-pinene and high-NO pinonaldehyde experiments are presented in Figure 5(b). Major products belonging to the $C_{10}H_{14}O_x$ and $C_{10}H_{15}NO_x$ family detected by both nitrate-CIMS (N) and amine-CIMS (A) are included. The data shown in ***Figure 5(b)*** represents averages over the first 320 s following the initiation of oxidation, corresponding to the early reaction stage, during which RO_2· + NO accounts for more than 90% of the total bimolecular RO_2· loss rate. In addition, all product signals here as well as all data used for comparison in the following paragraphs have been normalized by the pinonaldehyde turnover.

The pinonaldehyde turnover ratio during the first 320 s exceeded 5 and was substantially higher during the first 100 s. This large difference arises because pinonaldehyde was present at the start of the pinonaldehyde high-NO experiment and was therefore immediately available for reaction with ·OH. In contrast, under α-pinene high-NO conditions, pinonaldehyde had to be formed through α-pinene oxidation before it could undergo further reactions, resulting in a much lower pinonaldehyde turnover during the early stages of the experiment. For $C_{10}H_{15}O_x$·-related HOM detected by nitrate-CIMS the summed signals of the $C_{10}H_{14}O_x$ and $C_{10}H_{15}NO_x$ families under α-pinene high-NO conditions exceed those of pinonaldehyde high-NO conditions by factors of approximately 20 and 10, respectively. Although pinonaldehyde oxidation contributes to the formation of $C_{10}H_{15}O_x$·-related HOM under high-NO conditions, this contribution is

minor and can explain approximately 5% of the HOM yield observed from α-pinene oxidation. Similarly, for less oxygenated products measured by amine-CIMS, the summed concentrations of the $C_{10}H_{14}O_x$ and $C_{10}H_{15}NO_x$ families were 98 times higher in the α-pinene high-NO experiment, and 6.7 times higher in the pinonaldehyde high-NO experiment.

For highly oxygenated compounds detected by nitrate-CIMS, species containing more than 10 oxygen atoms account for 11% of the $C_{10}H_{14}O_x$ family and for 13% of the $C_{10}H_{15}NO_x$ family under α-pinene high-NO condition, whereas their contributions are much lower for pinonaldehyde high-NO conditions (3% and 5%, respectively).

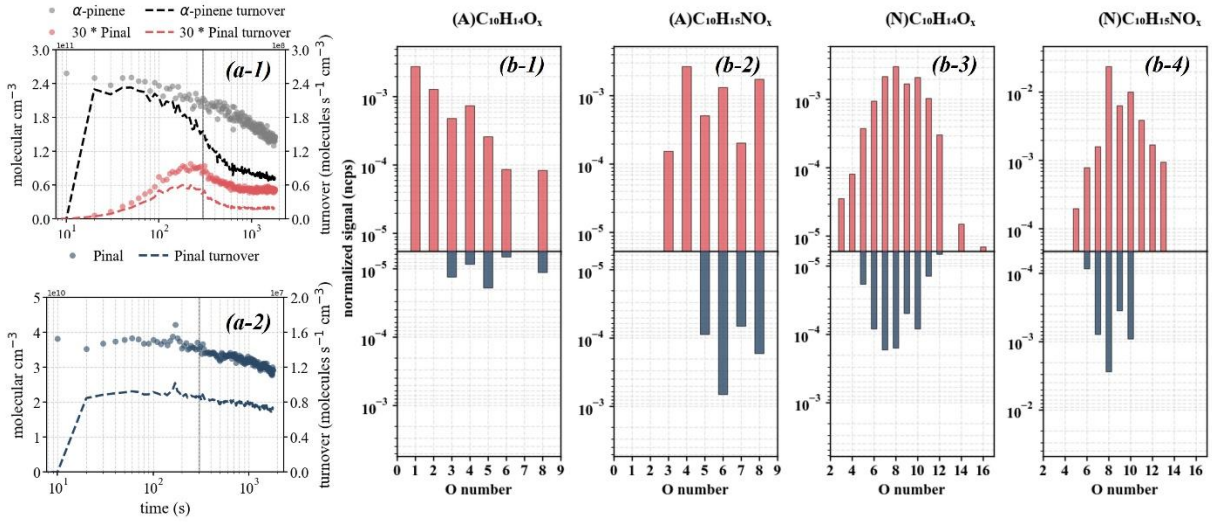

Figure 5. Panel (a-1) displays concentrations and turnover of α-pinene and pinonaldehyde (Pinal) during α-pinene photooxidation under high-NO conditions, while panel (a-2) represents concentrations and turnover of pinonaldehyde during the high-NO pinonaldehyde photooxidation experiment. Major product distributions are shown in panel (b-1) to (b-4). Signals detected in the pinonaldehyde experiment are normalized by the ratio of the pinonaldehyde turnover during the pinonaldehyde experiment to the respective turnover during the α-pinene experiment. The products are separated into four groups: (A)$C_{10}H_{14}O_x$, (A)$C_{10}H_{15}NO_x$, (N)$C_{10}H_{14}O_x$, (N)$C_{10}H_{15}NO_x$, of which (A) and (N) represent signals derived from amine-CIMS and nitrate-CIMS, respectively. Data from α-pinene oxidation and pinonaldehyde oxidation are colored in pink and blue, respectively.

We added a discussion about the reason why we observed a lower contribution of H-abstraction to total HOM formation (~30%) than the contribution from Shen et al., (2022) where they gained a contribution of up to 70%.

In the revised manuscript, we have expanded the discussion and now explicitly address several factors that may contribute to the discrepancy, including differences in reaction time, RO_2· fates under high-NO conditions, and instrumental setup. We attached following revised version:

The contribution of H-abstraction related products observed in this study was lower than that reported by Shen and coworkers, who reported a contribution of more than 70% (Shen et al., 2022). The experiments from the two studies were conducted in different chambers, under different conditions and with different instrumentations applied. Two chambers could introduce different wall losses of HOM, which can be further different between less oxygenated HOM and highly oxygenated HOM.

In this study the ·OH radicals were generated via photolysis of H_2O_2, whereas HONO photolysis was the main source of ·OH in Shen et al. (2022). The consecutive reaction between ·OH and H_2O_2 in our experiments leads to an enhanced production of HO_2· radicals, resulting in an HO_2· concentration of ~4×10^8 molecule cm^{-3}, which is approximately one order of magnitude higher than that reported by Shen et al. (2022). Also, the NO concentration in Shen et al. was constantly around ~20 ppb, while it was only ~7 ppb before reaction in our study, resulting in a concentration of ~1 ppb during the early-reaction stage. Despite these differences, the contributions of RO_2· + NO reactions are dominant in both studies, accounting for more than 95% of RO_2· biomolecular losses under high-NO conditions. In addition, we did only consider early reaction stages, during which secondary oxidation was negligible and RO_2· chemistry was dominated by autoxidation and RO_2· + NO reactions. Therefore, the chemical system can be expected to be similar for both studies, at least under high-NO conditions. However, the constantly higher level of NO in the study by Shen et al. (2022) may continuously promote the H-abstraction channel.

The discrepancy may also arise from differences in measurement techniques: Shen et al. (2022) used an Eisele type inlet (Mauldin et al., 1999), while in this study a MION inlet was used (Rissanen et al., 2019). To compare both inlet systems, we conducted an experiment where both types of inlets were simultaneously used to measure the same oxidation systems. The reference system was α-pinene oxidation by ·OH, with the addition of NO (***Figure S17).*** The results indicate that the MION inlets detects a larger fraction of lesser oxygenated HOM (less than eight oxygen atoms) than the Eisele inlet, and that these HOM dominate the $C_{10}H_{17}O_x$·-related HOM family, while the relative contribution of higher oxygenated HOM (more than eight oxygen atoms) was larger in the study by Shen et al. (2022). When only the highly oxygenated HOM compounds are considered as was done in the study be Shen and coworkers, the relative contribution of $C_{10}H_{15}O_x$·-related HOM to the total HOM does increase to 64%. Therefore, a deeper comparison of the two inlet types may be of interest in the future but is outside the scope of this study.

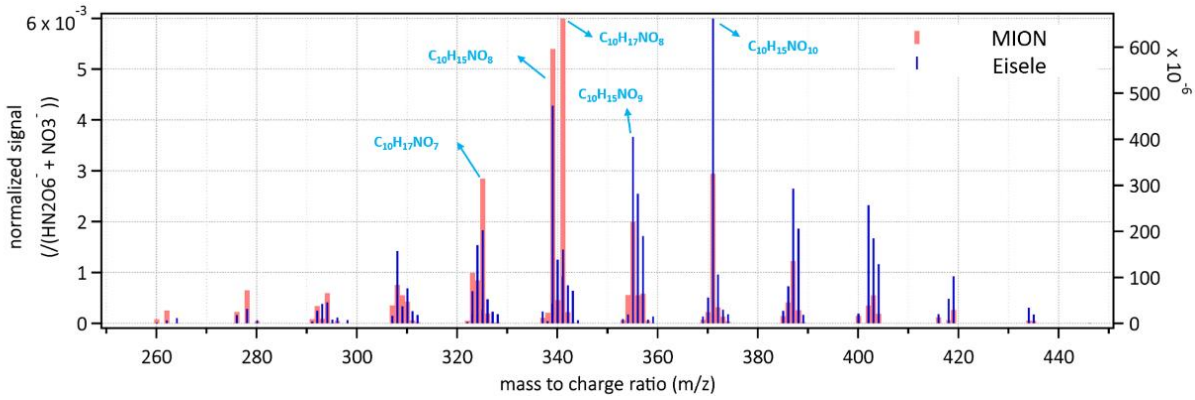

Figure S17. The signal of products derived from α-pinene oxidation with NO injection, detected by CIMS coupled with the MION (pink) and Eisele (blue) inlets.

Scientific Quality

The overall scientific quality is solid, as the hypothesis-experiment-interpretation logic does not show many shortcomings. There are two major comments I have.

> ***Comment 1:*** *Four-membered ring breakage with OH addition was mentioned in line 292, and the manuscript claimed the C10H17O7 unresponsiveness to NO change was due to this mechanism. There was no clear mechanism relationship explained in this manuscript and the paper referenced. A possible mechanistic interpretation is that the reaction rate of ring opening is fast with auto oxidation. This was partially mentioned in Lee et al., 2023., as the author stated the ring opening oxidation is a fast unimolecular reaction. This, however, is implicit, and the mechanistic linkage should be more explicitly developed within the manuscript.*

Responses:

We thank Shunyu Yao for this comment. We agreed with Shunyu Yao that this was not explained clearly enough in the previous version. The addition of an OH group to α-pinene can produce three isomers with the formula $C_{10}H_{17}O_3$. However, only one of these isomers will undergo subsequent autoxidation reactions after the four-member ring is opened (Xu et al., 2019). Furthermore, two subsequent autoxidation steps are needed to form $C_{10}H_{17}O_7$ peroxy radicals, and the rate constants of these autoxidation reactions are high enough to compete with biomolecule $RO_2\cdot$ reactions including $RO_2\cdot + NO$, $RO_2\cdot + HO_2\cdot$, and $RO_2\cdot + RO_2\cdot$. The rate constant of the $C_{10}H_{17}O_3$ autoxidation for forming $C_{10}H_{17}O_5$ is approximately 4 s^{-1}, while the $C_{10}H_{17}O_5$ autoxidation is even faster with approximately ~10 s^{-1} (Piletic and Kleindienst, 2022; Xu et al., 2019). For our experimental conditions the highest biomolecular reaction rate we could observe was ~1.88 s^{-1}, which is too low to efficiently compete with unimolecular reactions leading to the formation of $C_{10}H_{17}O_7$. Therefore, these previous studies can support our findings and we extended the discussion in the manuscript.

The updated discussion part is attached below:

The $C_{10}H_{17}O_7\cdot$ peroxy radicals exhibit a rapid formation rate and a high molar yield in α-pinene photooxidation systems, but their formation shows only a weak dependence on the NO concentration. Although ·OH addition to α-pinene yields three structural first-generation isomers ($C_{10}H_{17}O_3\cdot$), only the isomer that undergoes an opening of the four-membered ring forms a $C_{10}H_{17}O_3\cdot$ intermediate that is capable of subsequent autoxidation (Lee et al., 2023; Piletic and Kleindienst, 2022; Berndt et al., 2016). The ring-opened $C_{10}H_{17}O_3\cdot$ can then undergo two rapid unimolecular autoxidation steps, with a rate constant of approximately 4 s^{-1} for the first step which will lead to the formation of $C_{10}H_{17}O_5\cdot$, and a rate constant around 10 s^{-1} for the subsequent step and formation of $C_{10}H_{17}O_7\cdot$ species (Piletic and Kleindienst, 2022; Xu

et al., 2019). The fast autoxidation steps of the resulting peroxy radicals imply that the characteristic timescales of their formation are significantly shorter than those of competing bimolecular reactions with NO, RO_2, and HO_2, whose maximum effective rates in our experiments range from 0.02 to 1.88 s^{-1} under NO-free, low-NO, and high-NO conditions, respectively. Therefore, biomolecular reactions, particularly involving NO, cannot effectively compete with the rapid autoxidation reactions, which can explain the observed weak NO dependence of the formation of $C_{10}H_{17}O_7^{\cdot}$-related HOM.

Comment 2: *The lack of explanation introduced another question. Both OH addition and H-abstraction followed by oxidation would form alkyl peroxy radical. However NO seems to only affect the formation of C10H15Ox, the product from H-abstraction. The author used unimolecular reaction rate as explanation, but it does not fully answer why the formation of alkyloxy radicals is selective through mechanistic interpretation. The referenced paper does show explicitly ring opening steps and reaction rate reported. I believe it would be more helpful to include such data in this manuscript. Referring to the 2022 science publication, there were three types of ring opening structures with the same molecular composition (C10H15O3). I think the author should give more explanation on that park as well.*

Responses:

We agree with Shunyu Yao that the key issue is not whether NO promotes alkoxy radical formation in general, but why the influence of NO appears to be stronger for products originating from the H-abstraction pathway than for those formed via OH addition. As will be discussed below, these differences likely arise from the distinct structural constraints of the corresponding alkoxy radicals. In the H-abstraction pathway, alkoxy radical formation is required to initiate the HOM autoxidation chain through successive ring-opening reactions, whereas HOM formation through the OH-addition pathway can proceed by opening the four-membered ring and subsequent autoxidation without involvement of NO. The results of this study show that contribution of fragments (C7) was more important for the H-abstraction pathway than for the OH-addition pathway, which suggests that either alkoxy radical formation or subsequent decomposition is more efficient in the H-abstraction pathway. According to Shen et al. (2022), three distinct $C_{10}H_{15}O_3$ isomers can be generated through different ring-opening sequences. Subsequent reactions of these intermediates with NO lead to different alkoxy radicals, which are expected to exhibit different affinities toward H-migration, O_2 addition, and decomposition. Since the present measurements only provide molecular formulas, the individual contributions of these isomers cannot be resolved. Nevertheless, their coexistence may contribute to the uncertainty of the fate of alkoxy radicals and thus explain the observed low sensitivity of the related HOM formation towards NO.

For a more detailed explanation and discussion we extended the manuscript in section 3.2 as follows:

As shown in ***Figure S12***, the summed abundance of C_7 families ($C_7H_{(10,12)}O_x$, $C_7H_{(9,11)}NO_x$), increase accordingly with the increase the NO injection, accounting for 0.01%, 0.3% and 2.4% of HOM compounds under NO-free, low-NO and high-NO conditions, respectively. It indicated increasing alkoxy radical decomposition with increasing NO. C_7 fragments are formed via dissociation of C_{10} alkoxy radicals derived from bimolecular reactions of C_{10} peroxy radicals with NO. Thus, the presence of NO promotes C_7 fragments by enhancing the production of alkoxy radicals (Vereecken and Peeters, 2000; Berndt, 2021). As the most abundant families, $C_7H_9NO_x$ and $C_7H_{11}NO_x$, likely originate from decomposition of $C_{10}H_{15}O_{x-}$

$_1$· and $C_{10}H_{17}O_{x-1}$·, respectively. Under high-NO conditions, the ratio of $C_7H_9NO_x$ to $C_{10}H_{15}NO_x$ reached 0.22, substantially higher than the ratio of $C_7H_{11}NO_x$ to $C_{10}H_{17}NO_x$ (0.05). This observation suggests that either alkoxy radical formation or subsequent decomposition is more efficient in the H-abstraction pathway than in the ·OH-addition pathway.

Evidence for alkoxy radical H-migration is provided by the enhanced formation of $C_{10}H_{17}NO_7$ and $C_{20}H_{34}O_{11}$ under high-NO conditions (***Figure S9***). According to the oxygen-parity framework, $C_{10}H_{17}O_x$· radicals formed solely through autoxidation are expected to contain an odd number of oxygen atoms, whereas an alkoxy H-migration step changes the oxygen parity from odd to even (Kang et al., 2025). Thus, the observed increase in $C_{10}H_{17}NO_7$ and $C_{20}H_{34}O_{11}$ suggests the formation of $C_{10}H_{17}O_6$· peroxy radicals through at least one alkoxy radical isomerization step.

To initialize the HOM chain via OH-addition pathway, four-membered rings must open from chemically activated tertiary radicals, which is independent of NO (Xu et al., 2019). In contrast, HOM formation through the H-abstraction pathway requires NO. The initially formed peroxy radicals ($C_{10}H_{15}O_2$·) are unlikely to undergo autoxidation directly; therefore, their reaction with NO to form alkoxy radicals ($C_{10}H_{15}O$·), followed by the ring-opening step producing $C_{10}H_{15}O_3$· radicals, is necessary to initiate the HOM formation chain.

As autoxidation proceeds, higher oxygenated peroxy radicals, such as $C_{10}H_{17}O_x$· and $C_{10}H_{15}O_x$·, are formed from $C_{10}H_{17}O_3$· and $C_{10}H_{15}O_4$·, respectively. These peroxy radicals can further react with NO, yielding either the corresponding alkoxy radicals ($C_{10}H_{17}O_{x-1}$ and $C_{10}H_{15}O_{x-1}$) or organic nitrates ($C_{10}H_{17}NO_{x+1}$ and $C_{10}H_{15}NO_{x+1}$). However, the branching ratio between these two channels remains poorly constrained, contributing substantial uncertainty to the role of NO in HOM formation. Once formed, the fate of alkoxy radicals strongly depends on alkoxy radical structure (Vereecken and Peeters, 2010, 2009). Regardless of whether the precursor RO_2· radicals originate from the ·OH-addition or H-abstraction pathway, their subsequent chemistry can proceed through alkoxy radical intermediates. Therefore, the fate of these alkoxy radicals ultimately determines the impact of NO on HOM formation.

Overall, NO does influence HOM formation through alkoxy-radical chemistry. By promoting the conversion of RO_2· radicals to RO· radicals, NO initializes pathways for H-migration and decomposition that would otherwise be less important. The extent to which these processes enhance or suppress HOM formation depends strongly on the structures of both the peroxy and alkoxy radicals, introducing substantial uncertainty into the overall role of NO.

1. ***Presentation Quality***

The presentation quality of this manuscript is decent, with good paragraph structures, informative figures and mostly clear logical reasoning. I think figures can be improved with following comments:

Fig 1 should adopt structure-based illustrations to visualize free radical position and ring opening step.

Explanation between result and interpretation was compressed and information lacking. There are many cases where the author offered little to none detailed logic to obtain conclusions. This was briefly mentioned in the scientific quality part, but lack of explanation also hinders readers' interpretation of results.

Many terms are overly abbreviated, which creates confusion. For example, reaction conditions can have a full name instead of labeled as AN or PN. Reactions can also be written out instead of assigned identifiers in the very beginning of the manuscript.

Responses:

We thank Shunyu Yao for these comments and the suggestions to improve the figures. We have made several modifications accordingly.

1. A figure illustrating the structure of molecules and free radical positions was added, as shown in ***Figure S1***. It can help to understand the explanations for the reaction mechanisms in the following sections.

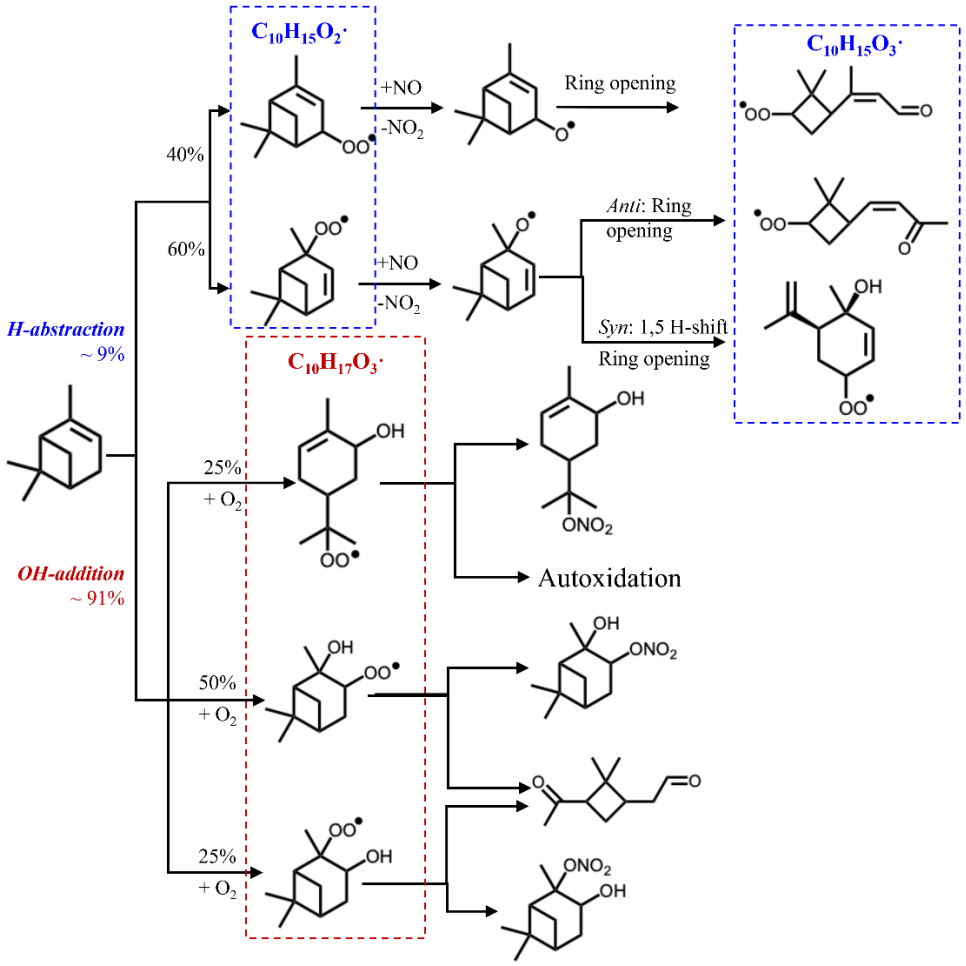

Figure S1. Formation pathways to form $C_{10}H_{15}O_3\cdot$ peroxy radicals through the H-abstraction channel and o form $C_{10}H_{17}O_3\cdot$ peroxy radicals through the OH-addition channel, derived from ·OH initiated α-pinene oxidation (Shen et al., 2022; Xu et al., 2019; Berndt et al., 2016).

2. Discussion was extended throughout the paper to link the observations and conclusions. Please find details in the ***responses*** to ***scientific significance and scientific quality part***.
3. All the abbreviations were replaced by full name throughout the paper:

   A0 was replaced by α-pinene (NO-free)

   AN_{low} was replaced by α-pinene (low-NO)

   AN_{high} was replaced by α-pinene (high-NO)

   P0 was replaced by pinonaldehyde (NO-free)

   PN_{high} was replaced by pinonaldehyde (high-NO)

   The changes can be found in ***Table 1***:

Table 1. Overview of experimental conditions: pinonaldehyde photooxidation without NO (NO-free) and with high NO (high-NO), α-pinene photooxidation without NO (NO-free), with low NO (low-NO), and

with high NO (high-NO). The precursor concentrations in the dark and in photooxidation steady-state conditions are shown at t_0 and t_S, respectively. The measurement uncertainty is less than 5%. Details about how to estimate ·OH and HO_2· radicals are given in Section 2.2.

		VOC		NO	·OH	HO_2·
		pinonaldehyde (ppbv)	α-pinene (ppbv)	(ppbv)	(# cm^{-3})	(# cm^{-3})
Pinonaldehyde (NO-free)	t_0	1.5	-	0	-	-
	t_S	0.75	-	0	6.5×10^6	6.4×10^8
Pinonaldehyde (high-NO)	t_0	1.8	-	7.0±0.13	-	-
	t_S	0.75	-	0.36±0.01	9.3×10^6	2.7×10^8
α-pinene (NO-free)	t_0	-	10.3±1.7	0	-	-
	t_S	0.01	8.3±1.4	0	1.25×10^6	3.1×10^8
α-pinene (low-NO)	t_0	-	11.1±1.3	0.91±0.05	-	-
	t_S	0.05	5.5±1.7	0.05±0.01	5.1×10^6	9.8×10^8
α-pinene (high-NO)	t_0	-	10.6±1.3	7.4±0.05	-	-
	t_S	0.09	4.2±2.1	0.16±0.01	7.5×10^6	1.0×10^9

Minor comments:

In Line 230, "with low NO (Anslow), and with high NO (Anlo)." Second Anlo should be ANhigh.

Responses:

Thanks for pointing out this mistake, it has been corrected.

In line 199, define ncps.

Responses:

Thanks for this comment, we now introduce this abbreviation properly:

A linear fit was applied to normalized $HO_2\cdot/[Br^- + (H_2O)Br^-]$ (in normalized counts per second, ncps) and modeled $[HO_2\cdot]_S$ (***Figure S4***), and the slope was used as calibration factor for calculating $HO_2\cdot$ levels in subsequent experiments (***Table 1***).

Line 369 "need longest time be formed." Consider rephrasing into longest formation time.

Responses:

Thanks for this comment, sentence was rephrased.

Hyphenation inconsistency, as an example both low-NO and low NO appeared.

Responses:

Thanks for this comment, all abbreviations and hyphenations have been corrected and should be now consistent throughout the manuscript.

References:

Baker, Y., Kang, S., Wang, H., Wu, R., Xu, J., Zanders, A., He, Q., Hohaus, T., Ziehm, T., Geretti, V., Bannan, T. J., O'Meara, S. P., Voliotis, A., Hallquist, M., McFiggans, G., Zorn, S. R., Wahner, A., and Mentel, T. F.: Impact of HO2⁄RO2 ratio on highly oxygenated α-pinene photooxidation products and secondary organic aerosol formation potential, Atmos. Chem. Phys., 24, 4789-4807, 10.5194/acp-24-4789-2024, 2024.

Berndt, T.: Peroxy Radical Processes and Product Formation in the OH Radical-Initiated Oxidation of alpha-Pinene for Near-Atmospheric Conditions, J Phys Chem A, 125, 9151-9160, 10.1021/acs.jpca.1c05576, 2021.

Berndt, T., Richters, S., Jokinen, T., Hyttinen, N., Kurten, T., Otkjaer, R. V., Kjaergaard, H. G., Stratmann, F., Herrmann, H., Sipila, M., Kulmala, M., and Ehn, M.: Hydroxyl radical-induced formation of highly oxidized organic compounds, NATURE COMMUNICATIONS, 7, 10.1038/ncomms13677, 2016.

Kang, S., Wildt, J., Pullinen, I., Vereecken, L., Wu, C., Wahner, A., Zorn, S. R., and Mentel, T. F.: Formation of highly oxygenated organic molecules from α-pinene photooxidation: evidence for the importance of highly oxygenated alkoxy radicals, EGUsphere, 2025, 1-33, 10.5194/egusphere-2025-2772, 2025.

Lee, B. H., Iyer, S., Kurtén, T., Varelas, J. G., Luo, J., Thomson, R. J., and Thornton, J. A.: Ring-opening yields and auto-oxidation rates of the resulting peroxy radicals from OH-oxidation of α-pinene and β-pinene, Environmental Science: Atmospheres, 3, 399-407, 10.1039/d2ea00133k, 2023.

Mauldin, R. L., Tanner, D. J., Heath, J. A., Huebert, B. J., and Eisele, F. L.: Observations of H2SO4and MSA during PEM-Tropics-A, Journal of Geophysical Research: Atmospheres, 104, 5801-5816, 10.1029/98jd02612, 1999.

Piletic, I. R. and Kleindienst, T. E.: Rates and Yields of Unimolecular Reactions Producing Highly Oxidized Peroxy Radicals in the OH-Induced Autoxidation of alpha-Pinene, beta-Pinene, and Limonene, J Phys Chem A, 126, 88-100, 10.1021/acs.jpca.1c07961, 2022.

Shen, H., Vereecken, L., Kang, S., Pullinen, I., Fuchs, H., Zhao, D., and Mentel, T. F.: Unexpected significance of a minor reaction pathway in daytime formation of biogenic highly oxygenated organic compounds, Science Advances, 8, eabp8702, doi:10.1126/sciadv.abp8702, 2022.

Vereecken, L. and Peeters, J.: Theoretical Study of the Formation of Acetone in the OH-Initiated Atmospheric Oxidation of α-Pinene, The Journal of Physical Chemistry A, 104, 11140-11146, 10.1021/jp0025173, 2000.

Vereecken, L. and Peeters, J.: Decomposition of substituted alkoxy radicals--part I: a generalized structure-activity relationship for reaction barrier heights, Phys Chem Chem Phys, 11, 9062-9074, 10.1039/b909712k, 2009.

Vereecken, L. and Peeters, J.: A structure-activity relationship for the rate coefficient of H-migration in substituted alkoxy radicals, Phys Chem Chem Phys, 12, 12608-12620, 10.1039/c0cp00387e, 2010.

Xu, L., Moller, K. H., Crounse, J. D., Otkjaer, R. V., Kjaergaard, H. G., and Wennberg, P. O.: Unimolecular Reactions of Peroxy Radicals Formed in the Oxidation of alpha-Pinene and beta-Pinene by Hydroxyl Radicals, J Phys Chem A, 123, 1661-1674, 10.1021/acs.jpca.8b11726, 2019.